International Tables for Crystallography (2006). Vol. C, Figure 2.3.1.11, p. 50.

2.3.1.1.7. *Axial divergence*

Divergence in the axial direction (formerly also called 'vertical divergence') causes asymmetric broadening and shifts the reflections. The aberration is illustrated in Fig. 2.3.1.11 for a low-2θ reflection in the transmission-specimen mode (Subsection 2.3.1.2). The narrow profile was obtained with $\delta = 4.4^\circ$ parallel slits placed between the monochromator and detector, and the broad profile with the slits removed. The slits caused a 33% reduction in peak intensity. This problem was recognized in the first design of the diffractometer using the X-ray tube line focus when parallel slits were used in the incident and diffracted beams to limit the effect (Parrish, 1949). Increasing the radius reduces the effect if the slit length is kept constant. The intensity is also reduced because the chord length intercepted is a smaller fraction of the longer radius diffraction cone. The construction of parallel (Soller) slits (Soller, 1924) is shown in Fig. 2.3.1.5(*d*).

The calculation of the aberration and the present status is summarized by Wilson (1963, pp. 40–45). The results depend on the aperture of the parallel slits, the length of the entrance and receiving slits, and 2θ. In the limit of small s, the shift of the centroid is

$$\Delta(2\theta, \text{rad}) = (s/l)^2 \cot 2\theta/6, \qquad (2.3.1.15)$$

where s is the spacing and l the length of the foils. The shift becomes very large at small 2θ's but not infinite as equation (2.3.1.15) implies. The shift is to smaller 2θ's in the forward-reflection region and to larger 2θ's in back-reflection. However, the mathematical formulation is difficult to quantify because in the forward-reflection region the axial divergence convolves with the flat-specimen aberration to increase the asymmetry. In the back-reflection region, the effect is not so obvious because the distortion is smaller and the Lorentz and dispersion factors also stretch the profiles to higher angles.

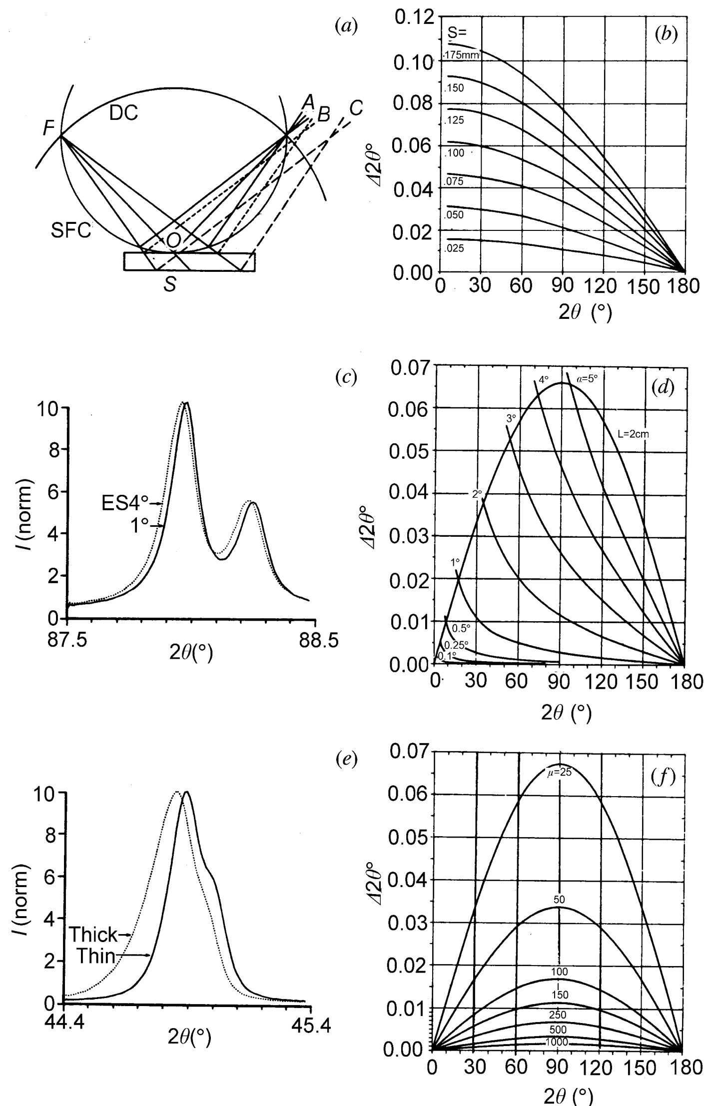

Fig. 2.3.1.10. (*a*) Origin of specimen-related aberrations in focusing plane of conventional reflection specimen diffractometer (Fig. 2.3.1.3). *A* no aberration from curved specimen; *B* flat specimen; *C* specimen displacement from 0. (*b*) Computed angular shifts caused by specimen displacement, $R = 185$ mm. (*c*) Flat-specimen asymmetric aberration, Si(422), Cu $K\alpha_1$, $K\alpha_2$ peak intensities normalized. (*d*) Computed flat-specimen centroid shifts for various apertures; parabola for constant irradiated 2 cm specimen length. (*e*) Transparency asymmetric aberration, LiF(200) powder reflection, Cu $K\alpha$, peak intensities normalized, thin specimen (solid-line profile) 0.1 mm thick; thick specimen (dotted-line profile) 1.0 mm, α_{ES} 1°, α_{RS} 0.046°. (*f*) Computed transparency centroid shifts for various values of linear absorption coefficient.

2.3.1.1.8. *Combined aberrations*

Additional aberrations are caused by inaccurate instrument set-up and alignment. For example, if the receiving-slit position is incorrect, the profiles are broadened. If, in addition, the incident beam is mis-centred or the θ–2θ is incorrect, a peak shift accompanies the broadening because the aberrations convolute, causing larger distortions and peak shifts than the individual aberrations, for example, flat-specimen, transparency, and axial divergence.

2.3.1.2. *Transmission specimen, θ–2θ scan*

Transmission-specimen methods are not as widely used as reflection methods but they provide important supplemental data and have advantages in a number of applications. Reflections occur from lattice planes oriented normal to the specimen surface rather than parallel. Reflection and transmission patterns can be compared to determine texture and preferred-orientation effects. The transmission method is better suited to the measurement of large d's. Smaller specimen volumes are required. The surface 'roughness' which may cause large intensity errors due to the microabsorption in reflection specimens is largely reduced.

The same basic diffractometer is used for both methods but the geometry is different because the diffracted beam continues to

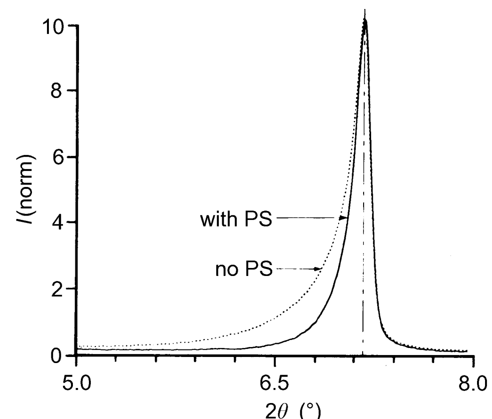

Fig. 2.3.1.11. Effect of axial divergence on profile shape. Narrow profile recorded with parallel slits (PS), $\delta = 4.4^\circ$ between monochromator and detector Fig. (2.3.1.12), and broad profile with these parallel slits removed. Faujasite, Cu $K\alpha$, α_{ES} 2°.

Copyright © 2006 International Union of Crystallography

references